Aust. J. Phys., 1983, 36, 565–72

# A Fast-response EBIC System*

C. J. Rossouw, F. J. Maher and A. A. Panjkov

Division of Chemical Physics, CSIRO, P.O. Box 160, Clayton, Vic. 3168.

*Abstract*

The application of the EBIC technique in the study of electrical activity of defects in semiconductors is discussed, with particular reference to instrumentation. A fast-response current amplifier, built in our Division, is shown to be more than adequate for most EBIC applications. Some examples of EBIC analysis are presented.

## 1. Introduction

The electron beam-induced current (EBIC) mode of analysis in the scanning electron microscope (SEM) yields information on the electrical characteristics of defects near the surface of a suitable semiconductor or insulator on a sub-micron scale. This technique, described in the literature as early as 1964 by Everhart *et al.*, has recently been included in a broad description of EBIC phenomena in a book by Ehrenberg and Gibbons (1981). Development and refinement of the technique over the past two decades has led, for instance, to the quantitative measurement of the electrical activity of crystal defects, such as well-characterized dislocations in silicon (Ourmazd and Booker 1979) and measurements of minority carrier diffusion lengths (Ioannou and Davidson 1979). The present paper provides a basic introduction to the EBIC technique for the non-specialist reader. It is hoped that the emphasis on instrumentation, based on some recent experimental work, will help as a practical guide for the design and implementation of such a facility. We refer to Leamy *et al.* (1978) for a far more complete introduction to the subject.

We have seen the need for an EBIC facility to complement studies on p–n junctions which have been locally fabricated by ion implantation. The EBIC facility is useful in assessing the effectiveness of various annealing procedures (thermal, laser, electron beam) in electrically activating the dopant by epitaxial regrowth of the amorphized implanted layer. This is a general facility open to the Australian Ion Implantation Research Group, a body created to help coordinate and establish cooperation in this area of research between institutions such as the RMIT, the CSIRO Division of Chemical Physics and the AAEC at Lucas Heights.

* Paper presented at the Seventh AIP Solid State Physics Meeting, Wagga Wagga, N.S.W., 9–11 February 1983.

0004-9506/83/040565$02.00

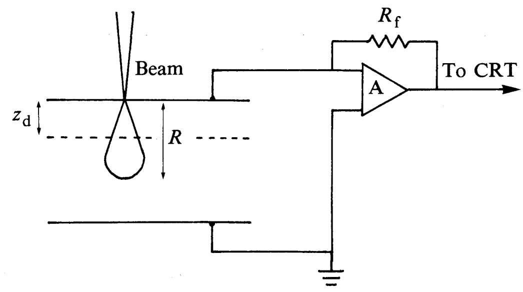


**Fig. 1.** Experimental setup for an EBIC specimen in an SEM, showing the external circuit for EBIC.

## 2. Generation of EBIC

An energetic electron beam is used to inject charge carriers within a pear-shaped generation volume immediately beneath the target surface. The energy dissipation profile depends on beam energy, target material and geometrical considerations (see Donolato 1981). Fig. 1 illustrates the circuit for EBIC generation in an SEM. The penetration (or range) $R$ for electrons with energies of 5–25 keV may be expressed in the form

$$R = \alpha E_0^\beta , \tag{1}$$

where $E_0$ is the beam energy and $\alpha, \beta$ are constants which depend on the target material (Everhart and Hoff 1971). For silicon we have $\alpha \approx 0{\cdot}02$ and $\beta \approx 1{\cdot}7$ if $E_0$ is measured in keV and $R$ in $\mu$m. The injection of charge carriers to depths of between $0{\cdot}3$–$5\ \mu$m may readily be achieved. In the absence of an intrinsic electric field, the electron–hole pairs rapidly annihilate and no EBIC is registered in the external circuit.

Now consider a depletion layer on the top surface of a semiconductor, perhaps due to an existing planar p–n junction. Alternatively, the depletion layer may be due to a Schottky barrier formed by the evaporation of a thin metallic film on the top surface (e.g. Au on n-type Si, Ag or Al on p-type Si). The depth $z_d$ of the Schottky barrier depletion region may be written as

$$z_d = A(\rho v)^{\frac{1}{2}} , \tag{2}$$

where $v$ is the sum of the Schottky barrier potential (normally $0{\cdot}5$–$0{\cdot}8$ V) and an optional applied reverse bias, $\rho$ is the sheet resistivity of the semiconductor in $\Omega$ cm, $A$ is a constant ($\approx 0{\cdot}5$ for Si) and $z_d$ is in $\mu$m.

Within the depletion zone, the intrinsic electric field sweeps the electrons and holes in opposite directions, leading to EBIC in the external circuit. This signal is amplified and displayed on the SEM monitor screen, where the EBIC may be recorded as an $x$–$y$ line trace or a brightness modulated SEM micrograph. The magnitude of the EBIC may be written as

$$\mathrm{EBIC} = C I_b E_0 / \varepsilon , \tag{3}$$

where $I_b$ is the incident beam current, $\varepsilon$ is the energy required to create an electron–hole pair ($3{\cdot}6$ eV for Si at room temperature), and $C$ is a constant between 0 and 1 which is related to the charge collection efficiency across the depletion zone and competing energy loss mechanisms (see Gedcke *et al.* 1978). The number of charge carriers created per incident electron is typically of order $10^3$. The target thus acts as its own solid state signal detector and amplifier.

Under certain conditions, a reduced EBIC indicates the presence of electrically active recombination centres within the depletion zone. These may be due to the presence of extended crystal defects introduced for example by epitaxial regrowth after ion implantation, by diffusion, by high temperature plastic deformation, or by localized variations in dopant concentration and activity. The modulation is typically 1–5% of the total EBIC. Thus, to obtain black to white contrast from these small variations on an SEM monitor screen, it is often necessary to apply a DC offset to the EBIC and increase the overall gain of the amplifier.

## 3. Amplifier Design

In setting up the EBIC facility, we designed the amplifier in Fig. 1 to be compatible with our Hitachi 405A SEM. Briefly, $3 \times 10^5$ pixels per frame are resolved on the monitor screen, the pixel area being about $0 \cdot 2 \times 0 \cdot 2$ mm. Thus for rapid scanning ($0 \cdot 5$ s per frame) a 600 kHz bandwidth is desirable. A 2 V swing is sufficient to drive the monitor intensity over its full range. With $I_b$ of order $10^{-8}$–$10^{-11}$ A and EBIC $\approx 10^3 I_b$, a sensitivity of about $10^6$–$10^9$ V A$^{-1}$ is necessary. Amplifier design must represent a compromise between sensitivity and tolerable noise, which is essentially determined by the bandwidth $\Delta f$ of the amplifier. This amplifier was constructed from ultra-fast FET operational amps, and has a maximum sensitivity of $3 \times 10^8$ V A$^{-1}$ and bandwidth $\Delta f = 600$ kHz (see Maher and Rossouw 1983 for a complete description and circuit diagram). The most significant noise is generated in the input stage, where the amplification ($10^5$ V A$^{-1}$) is equivalent to a feedback resistor of $R_f = 10^5\ \Omega$. The r.m.s. thermal noise current $\sigma_{rms}$ generated at a temperature $T$ is given by (see Motchenbacher and Fitchen 1973)

$$\sigma_{rms} = (4k_B T \Delta f / R_f)^{\frac{1}{2}}, \tag{4}$$

with a value of $3 \cdot 1 \times 10^{-10}$ A at room temperature. A bench test of the amplifier has confirmed this value. In practice the noise introduced by specimen capacitance tends to override this value, so that EBIC images tend not to be degraded by amplifier characteristics, but rather by specimen noise and response time.

Our purpose-built amplifier compares very favourably with other current amplifiers with regard to noise and, in particular, bandwidth. The fast scan time enables rapid optimization of DC offset, incident beam current etc. while viewing the EBIC image. This is of great advantage compared with scan times of $\geqslant 500$ s necessary with commonly used electrometer amplifiers with slow rise-times, for example, the Keithley 427A (Cath and Peabody 1971). Noise is further reduced by switching in a 12 kHz filter when the 50 s per frame necessary for photographic recording is used.

## 4. Some Applications of EBIC

Fig. 2*a* shows a conventional secondary electron image of a transistor in the SEM, with surface topography related to masking and oxide growth during device manufacture. The EBIC images in Figs 2*b* and 2*c* display the projection of base–emitter and base–collector junctions on the top surface. Variation of EBIC with $E_0$ yields information on the depth of the junction beneath the overlay material (see Gonzales 1974). If $E_0$ is increased, a greater depth penetration is achieved, and the EBIC may also be increased depending on the depletion layer depth and the mobility and lifetime of the charge carriers. However, this decreases the spatial resolution of the technique in bulk specimens, and the relative modulation of the EBIC by crystal defects is also reduced.

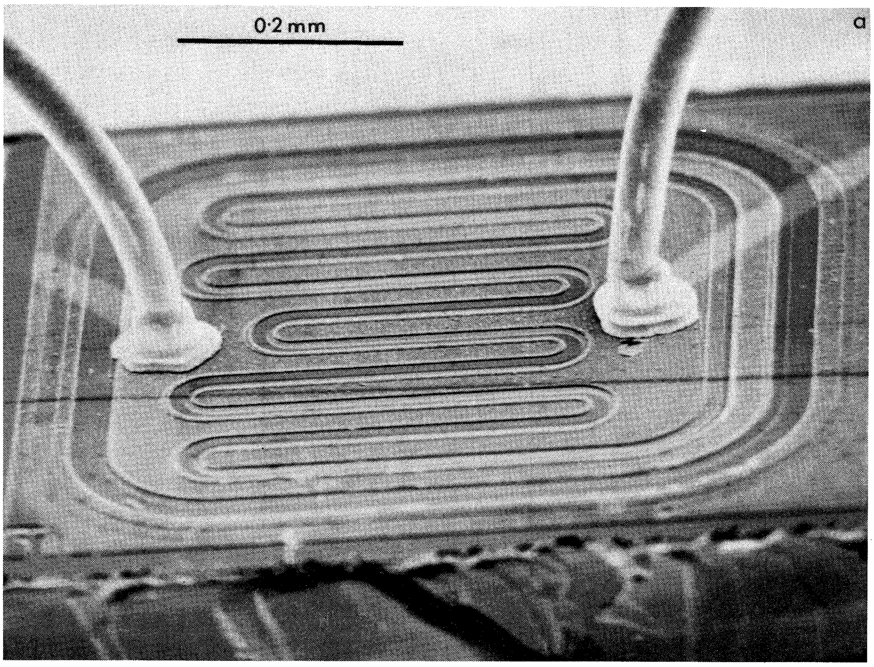


**Fig. 2.** NPN transistor imaged in (*a*) the secondary electron mode and the EBIC mode showing (*b*) base–emitter and (*c*) base–collector junctions. Here the beam energy $E_0$ is 15 keV.

Fig. 3 shows a typical EBIC micrograph of a locally produced solar cell, where a DC offset and increased amplification have been used to image electrically active line defects (dislocations). Here black-to-white contrast represents approximately a 5% variation in total EBIC, the 5 keV beam enabling a spatial resolution of about 0·5 $\mu$m. These defects adversely affect the performance of such a cell. It has been shown by deep level transient spectroscopy that the electrical activity of dislocations can be passivated by the diffusion of atomic hydrogen (Pohoryles 1981). Preliminary results in our Division using the EBIC technique to monitor the effect of hydrogenation of dislocations in silicon have been encouraging, and work on this aspect is progressing.

A comparison of various annealing procedures for activating a junction in implanted Si has been given by Mizuta *et al.* (1981) using the EBIC technique. They found electron beam annealing to be generally superior to laser annealing with respect to lateral and depth homogeneity in electrical characteristics. Fig. 4 shows an EBIC image from an implanted Si wafer, where a laser spot anneal has been used to activate the implant. Here the 1 $\Omega$cm p-type wafer was implanted with 30 keV $As^+$ ions to a dose of $10^{15}$ cm$^{-2}$. The transition between the electrically active and inactive regions at the edge of the laser spot is relatively sharp, but gross variations in the lateral uniformity of the junction within the annealed region is evident on a scale of about 3 $\mu$m.

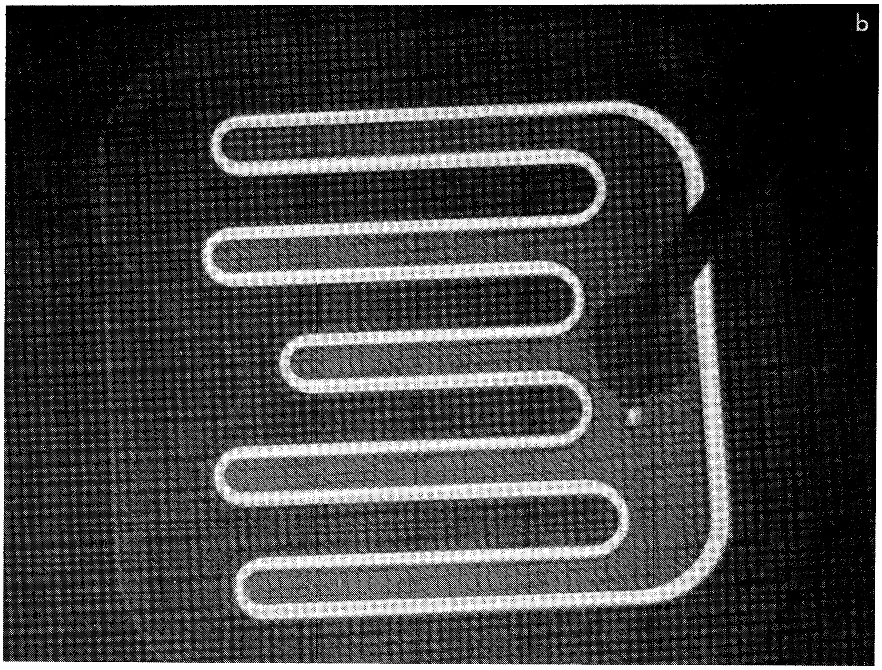


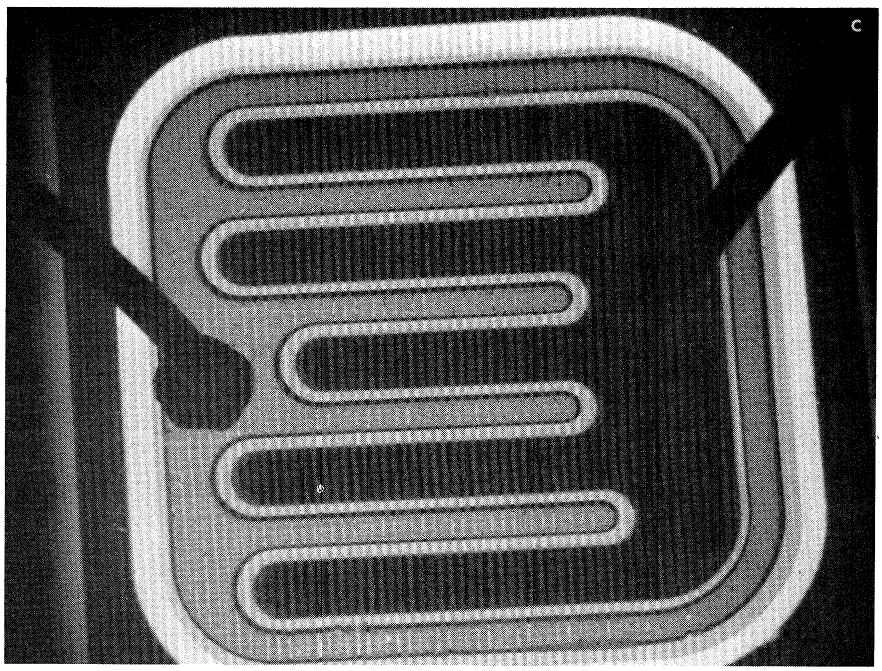


**Figs 2*b* and 2*c*.** [*See opposite page*]

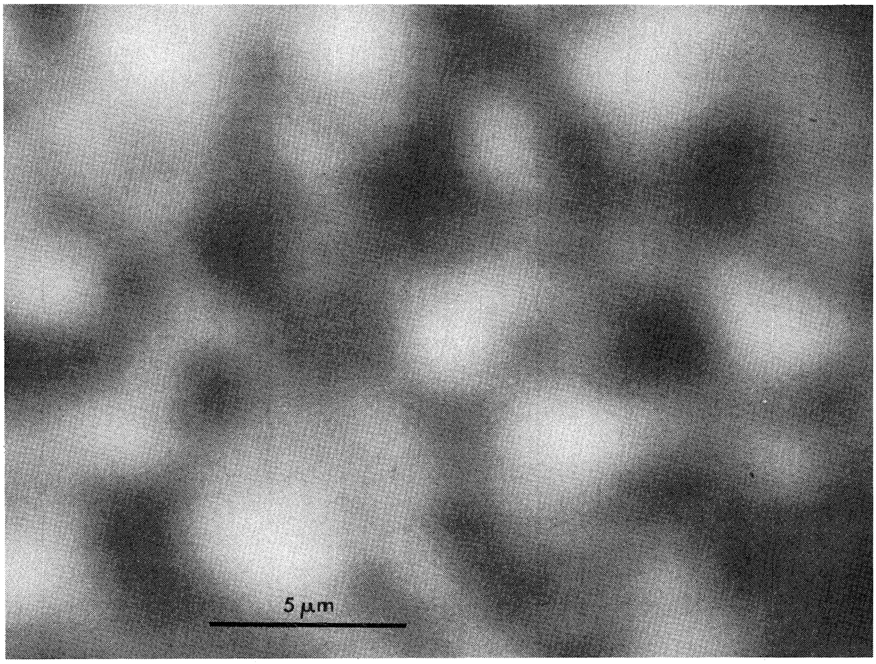


**Fig. 3.** EBIC image (inverted contrast) from the top surface of a solar cell, with $E_0 = 5$ keV.

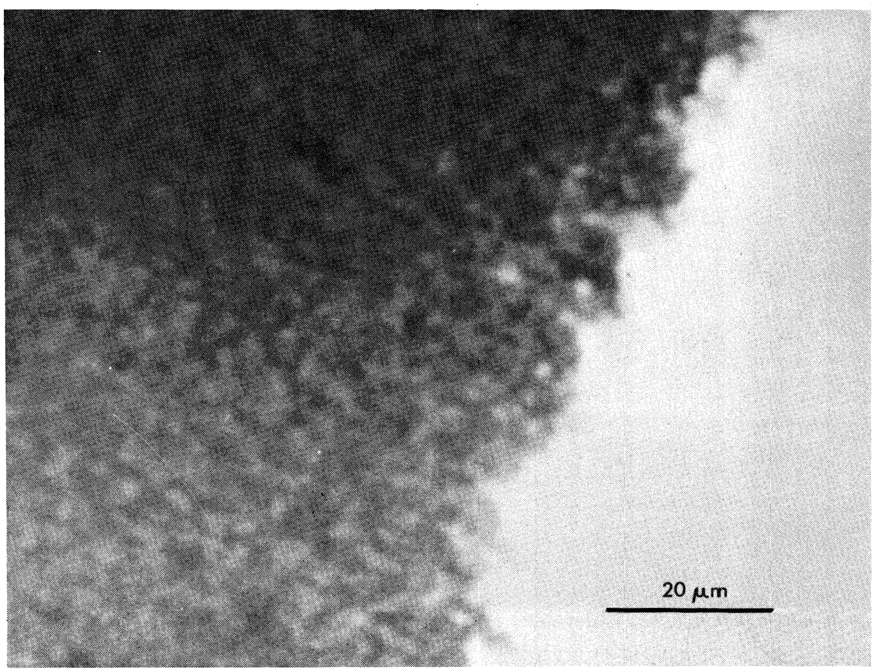


**Fig. 4.** EBIC image (inverted contrast) of laser-annealed silicon implanted with $As^+$ showing the edge of the laser spot, and the unannealed region on the right-hand side. Here $E_0$ is 15 keV.

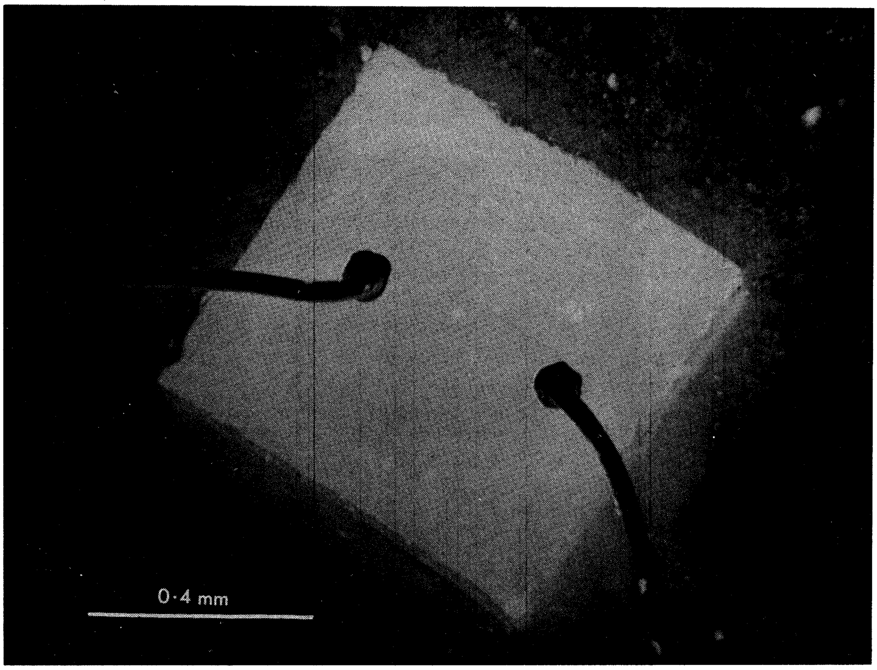


**Fig. 5.** Backscattered electron image (inverted contrast) of a transistor using a solar cell detector, with $E_0 = 25$ keV. Note the difference in contrast between the gold leads and the Si substrate.

## 5. Concluding Remarks

The purpose-built EBIC amplifier costs about $150 for all components, which is an order of magnitude cheaper than suitable commercially available electrometers. The good response time from rather large chunks of solar cell in the EBIC mode prompted us to install an off-the-shelf solar cell ($9·95 from most electronics retailers) as a backscattered electron detector. An example of a backscattered electron image obtained is shown in Fig. 5. This certainly provides a cheap though somewhat noisy alternative to some solid state detectors available for this purpose. A requirement for low output noise is that the intrinsic resistance of the detector be comparable with or greater than the equivalent feedback resistance of the input stage of the amplifier. In this respect surface barrier detectors are superior to low resistance p–n junctions.

In the measurement of contrast variations of about 0·5% across electrically active defects, noise generated in the specimen can present problems. This can be substantially reduced by encoding the EBIC signal by means of phase-sensitive detection, i.e. a lock-in amplifier tuned in to a high-frequency electron beam chopping system (Ourmazd *et al.* 1981). Alternative means for lessening the effects of specimen noise on the EBIC are presently being investigated.

## Acknowledgment

One of us (A.A.P.) would like to thank the CSIRO Division of Chemical Physics for providing a studentship.

## References

Cath, P. G., and Peabody, A. M. (1971). *Anal. Chem.* **43**, 91A.

Donolato, C. (1981). *Phys. Status Solidi* (*a*) **66**, 445.

Ehrenberg, W., and Gibbons, D. J. (1981). 'Electron Bombardment Induced Conductivity and Its Applications', p. 294 (Academic: London).

Everhart, T. E., and Hoff, P. H. (1971). *J. Appl. Phys.* **42**, 5837.

Everhart, T. E., Wells, O. C., and Matta, R. K. (1964). *J. Electrochem. Soc.* **111**, 929.

Gedcke, D. A., Ayers, J. B., and DeNee, P. B. (1978). *In* 'Scanning Electron Microscopy', Vol. 1 (Ed. O. Johari), p. 581 (SEM Inc: Chicago).

Gonzales, A. J. (1974). *In* 'Scanning Electron Microscopy' (Eds O. Johari and I. Covin), p. 941 (ITT Research Institute: Chicago).

Ioannou, D. E., and Davidson, S. M. (1979). *J. Phys.* D **12**, 1339.

Leamy, H. J., Kimerling, L. C., and Ferris, S. D. (1978). *In* 'Scanning Electron Microscopy', Vol. 1 (Ed. O. Johari), p. 717 (SEM Inc: Chicago).

Maher, F. J., and Rossouw, C. J. (1983). Design and performance of an amplifier for EBIC imaging in a scanning electron microscope. *J. Phys.* E (in press).

Mizuta, M., Sheng, N. H., and Merz, J. L. (1981). *J. Appl. Phys.* **52**, 6437.

Motchenbacher, C. D., and Fitchen, F. C. (1973). 'Low Noise Electronic Design', p. 10 (Wiley: London).

Ourmazd, A., and Booker, G. R. (1979). *Phys. Status Solidi* (*a*) **55**, 771.

Ourmazd, A., Wilshaw, P. R., and Cripps, R. M. (1981). 'Electron Microscopy and Analysis 1981', Inst. Phys. Conf. Ser. No. 61, p. 519 (Institute of Physics: London).

Pohoryles, B. (1981). *Phys. Status Solidi* (*a*) **67**, K75.

Manuscript received 18 January, accepted 7 April 1983